World Electric Vehicle Journal

MDPI

Article

Analysis of Active Suspension Control Based on Improved Fuzzy Neural Network PID

Mei Li *, Jiapeng Li, Guisheng Li and Jie Xu

Mechanical and Electrical Engineering College, Hainan University, Haikou 570100, China
* Correspondence: meili@hainanu.edu.cn

Abstract: To improve the comfort and smoothness of vehicle driving and reduce the vehicle vibration caused by uneven road surface. In this paper, a new active suspension control strategy is pro-posed by combining a fuzzy neural network and a proportional-integral-derivative (PID) controller, taking body acceleration as the main optimization target and adjusting the parameters of the PID controller in real time. Meanwhile, a fuzzy neural network parameter optimization algorithm combining a particle swarm optimization algorithm and gradient descent method is proposed to realize offline optimization and online fine-tuning of fuzzy neural network parameters. Finally, the active suspension model of a 2-degree-of-freedom 1/4 vehicle is established using MATLAB/Simulink, and the proposed control scheme is verified through simulation studies. The results show that the active suspension system with a particle swarm-optimized fuzzy neural network control method improves the spring mass acceleration, dynamic deflection of suspension, and dynamic tire deformation by 30.4%, 17.8%, and 15.5%, respectively, compared with the passive suspension. In addition, there are also 14.6%, 12.1%, and 11.2% performance improvements, respectively, compared to the PID-controlled active suspension system. These results indicate that the control strategy proposed in this paper can improve the vehicle driving performance and can support the design and development of active suspension systems.

Keywords: fuzzy neural network; particle swarm algorithm; PID control; active suspension; MATLAB/Simulink simulation

Citation: Li, M.; Li, J.; Li, G.; Xu, J. Analysis of Active Suspension Control Based on Improved Fuzzy Neural Network PID. *World Electr. Veh. J.* **2022**, *13*, 226. https://doi.org/10.3390/wevj13120226

Academic Editors: Yong Li, Xing Xu, Lin Zhang, Yechen Qin and Yang Lu

Received: 6 October 2022
Accepted: 2 November 2022
Published: 24 November 2022

1. Introduction

The suspension system's qualities determine the vehicle's smoothness and handling stability [1]. Traditional passive suspension systems have fixed parameters such as stiffness and damping, so they cannot effectively suppress vehicle vibration in the face of complex driving conditions. In order to reduce body vibration brought on by outside disturbances and give passengers a comfortable ride experience under various driving conditions, the active suspension can adjust the vehicle suspension in real time through active control force according to the road condition information [2–4].

For the controller design and optimization of active suspension systems, many researchers have proposed some simple and feasible control methods, such as linear quadratic regulator (LQR) control, PID control, optimal control, adaptive control, and sliding mode control [5–8]. Among them, PID control is favored by many researchers due to its relatively mature technology and wide application market. The traditional proportional-integral-derivative (PID) controller has the advantages of simple structure, good real-time performance, and low cost [9]. However, in today's practical engineering applications, many new control strategies have good improvements compared to PID control [10]. The parameters of the traditional PID controller are difficult to set accurately and are fixed after setting, and they cannot adapt to all suspension conditions as the vehicle working conditions change in real time [11].

In order to be able to improve the control effect of the PID controller, much in-depth research has been carried out. For example, fuzzy control is used to correct the PID

parameters, allowing the PID parameters to vary in real time within a specific range, improving the accuracy of the controller [12]. In the literature [13], a type of PID transverse interconnected electronically controlled air suspension system controller based on an optimization algorithm has been designed, and the optimal solution of PID controller parameters obtained. In addition, the highly parallel structure and powerful learning capability of the neural network system can also be well used to achieve online real-time adjustment of PID parameters [14–16]. It can be seen that, by combining different optimization strategies with PID control and real-time optimization of PID controller parameters, better control results can be achieved. However, a single optimization strategy also has certain defects; for example, fuzzy control has a strong subjectivity and uncertainty, which can be considered as a subjective means of expressing domain expert knowledge, and as the number of fuzzy rules increases, the parameters and structure of this control system will become increasingly difficult to establish. Neural network control is also not perfect, and there are many drawbacks in practical applications, such as the uncontrollability of network behavior, convergence and stability being difficult to guarantee, and multiple instances of trial and error being needed for the network.

It was found that hybrid control has better results for PID controllers compared to a single optimization strategy. Based on the 14-degree-of-freedom whole vehicle model, in [17], two control systems, the fuzzy PID controller and the neural network controller, have been used to substantially improve lateral stability and vehicle handling. In addition, in [18], the fuzzy road information is collected in real time and used to adjust the control performance of the fuzzy PID, so as to develop a new road condition-based fuzzy PID control strategy that meets the control performance requirements under different road conditions. A vibration-controlled active suspension based on an adaptive fuzzy fractional-order PID controller is proposed in [19], which was very effective in reducing driver body vibrations, thus improving the ride quality of the driver. In order to optimize the control system, an attempt was made in [20] to optimize the PID controller and Fuzzy PID controller using a particle swarm optimization (PSO) algorithm with excellent efficiency in reducing the vertical displacement of the body and obtaining a suitable control signal.

In addition to achieving active suspension control through a combination of control methods, a new control method with better performance has been proposed by combining fuzzy control theory and neural network control theory. In a sense, this design approach does not have the same heavy reliance on expert experience as fuzzy control, while retaining the adaptive performance and learning capability of neural network control. For example, the Adaptive Neuro-Fuzzy Inference System (ANFIS) is an artificial neural network integrated fuzzy logic control system whose control rules are obtained by implementing the Sugeno first-order fuzzy inference system in the form of a network. In [21], a comparison of the control of a semi-vehicle suspension system using PID, LQR, FUZZY, and ANFIS controllers was analyzed, and it was found that the ANFIS controller provided the best performance in terms of "stabilization time" and "peak overshoot". Meanwhile, in [22], a fuzzy control and neuro-fuzzy inference system was tested; the solenoid valve was controlled by an ANFIS, and the proposed method improved the ride comfort while maintaining road safety. The latter was a fuzzy neural network composed of an RBF neural network model, whose biggest advantage is that the fuzzy inference process and the RBF function have functional equivalence and are suitable for real-time control of the system. In [23], a Takagi–Sugeno fuzzy controller was designed to control the contraction–expansion factor to satisfy the control input current of the MR damper by introducing a fuzzy neural network controller with PSO and BP learning and training algorithms, and the results showed that the system approach was effective. For the regulation of the PID controller, an effective real-time control strategy is needed. Therefore, this paper proposes an active suspension control strategy based on particle swarm optimization with fuzzy neural network PID control. The real-time control performance of the fuzzy neural network is used to achieve the rectification of the PID controller parameters for the purpose of real-time control of the suspension system. However, the fuzzy neural network has many parameters such

as center, width, and weights, and it is difficult to obtain a reliable set of parameters. For this reason, the particle swarm optimization method is used to calculate a set of optimal parameters offline based on the objective function. In addition, it can avoid the problem that the neural network using gradient descent method may lead to gradient explosion, or the network not being able to converge for a long time due to too large or too small optimization weights [24]. Through MATLAB/Simulink simulation, it is shown that the FNN-PID control strategy of particle swarm optimization has a certain control effect on the active suspension system.

The rest of this paper is organized as follows. In Section 2, the mathematical model of the active suspension system for a 2-degree-of-freedom 1/4 vehicle and the road excitation model are presented, and the principles of PID control and fuzzy neural network PID control, as well as the combined optimization algorithm of particle swarm optimization algorithm and gradient descent method, are introduced. In Section 3, the simulation results of the suspension system controller design are shown. Finally, the conclusion and summary are presented in Section 4.

2. Materials and Methods

2.1. Active Suspension Simulation Model

The 2-degree-of-freedom 1/4 suspension model is shown in Figure 1, and the following assumptions are made regarding the model.

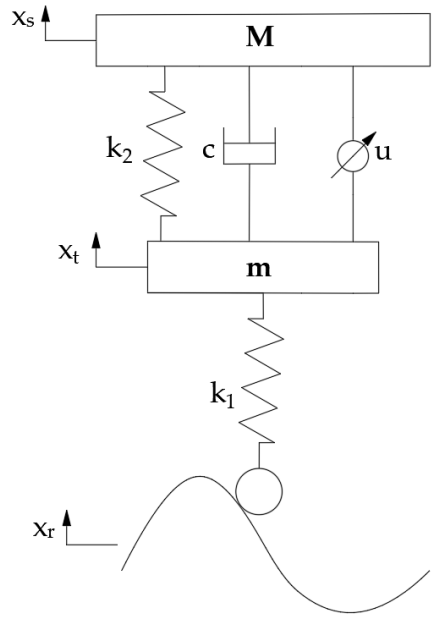

Figure 1. 2-degree-of-freedom 1/4 active suspension model.

1. The elastic center of the vehicle body coincides with the center of mass;
2. The vehicle body is rigid, and the occupants move in the same way as the vehicle body;
3. There is no sliding between the tires and the road, and the wheels are always in contact with the ground;
4. The vertical vibration characteristics of the wheel are reduced by a spring that does not take into account the damping effect.

As shown in Figure 1, M denotes the mass on the spring and m denotes the mass under the spring; x_r denotes the road disturbance excitation, x_t denotes the vertical displacement of the mass under the spring, and x_s denotes the vertical displacement of the mass on the spring; c denotes the suspension equivalent damping; k_1 is the tire equivalent stiffness and k_2 is the suspension stiffness; and u is the actuator active control force.

According to Newton's second law, combined with the suspension system dynamics model, the 1/4 active suspension dynamics equation is established as follows:

$$M\ddot{x}_s + k_2(x_s - x_t) + c(\dot{x}_s - \dot{x}_t) - u = 0 \tag{1}$$

$$m\ddot{x}_t - k_1(x_r - x_t) - k_2(x_s - x_t) - c(\dot{x}_s - \dot{x}_t) + u = 0 \tag{2}$$

Meanwhile, the state variable is selected as: $x_1 = x_s - x_t$, $x_2 = \dot{x}_s$, $x_3 = x_r - x_t$, $x_4 = \dot{x}_t$. The state vector is $X = [x_1\ x_2\ x_3\ x_4]^T$. The output variable is $y_1 = \dot{x}_2 = \ddot{x}_s$, $y_2 = x_1 = x_s - x_t$, $y_3 = x_3 = x_r - x_t$. The output vector is represented as $Y = [y_1\ y_2\ y_3]^T$. The input vector is $U = [u\ x_r]^T$.

Then, the state equation of the model is shown in (3).

$$\begin{cases} \dot{X} = AX + BU \\ Y = CX + DU \end{cases} \tag{3}$$

Among them, $A = \begin{bmatrix} 0 & 1 & 0 & -1 \\ -\frac{k_2}{M} & -\frac{c}{M} & 0 & \frac{c}{M} \\ 0 & 0 & 0 & -1 \\ \frac{k_2}{m} & \frac{c}{M} & \frac{k_1}{m} & -\frac{c}{M} \end{bmatrix}$, $B = \begin{bmatrix} 0 & 0 \\ \frac{1}{M} & 0 \\ 0 & 1 \\ \frac{1}{M} & 0 \end{bmatrix}$, $C = \begin{bmatrix} -\frac{k_2}{M} & -\frac{c}{M} & 0 & \frac{k_2}{M} \\ 1 & 0 & 0 & 0 \\ 0 & 0 & 1 & 0 \end{bmatrix}$, $D = \begin{bmatrix} \frac{1}{M} & 0 \\ 0 & 0 \\ 0 & 0 \end{bmatrix}$.

2.2. Road Excitation Model

2.2.1. White Noise Road Excitation

The difference between different grades of road mainly lies in the difference in road roughness, which is generally expressed by the road unevenness coefficient, G_q. According to the "Draft Method for Representation of Road Unevenness" presented by the International Organization for Standardization in ISO/TC108/SC2N67, the power spectrum density of a road can be expressed as follows [25]:

$$G_q(n) = G_q(n_0)\left(\frac{n}{n_0}\right)^{-w} \tag{4}$$

In the formula, n is the spatial frequency, n_0 is the reference spatial frequency, $n_0 = 0.1\ m^{-1}$, $G_q(n_0)$ is the reference spatial frequency of the road power spectral density, and w is the frequency index, often taken as $w = 2$.

For the analysis of vehicle suspension system dynamics, the vehicle travel speed is also a factor to be considered [26]. Converting the spatial frequency power spectral density, $G_q(n)$, to the temporal frequency power spectral density, $G_q(f)$, the variable of vehicle speed can be introduced. When a vehicle travels at a certain speed on a road surface with spatial frequency n, its equivalent time frequency can be expressed as:

$$f = vn \tag{5}$$

In the formula, v is the speed of the vehicle in $m \cdot s^{-1}$ and f is the time frequency in s^{-1}.

As a result, the following may be deduced about the road excitation model created using the filtered white noise method:

$$\dot{x}(t) + 2\pi f_0 x(t) = 2\pi n_0 \sqrt{G_q(n_0)v}W(t) \tag{6}$$

In the formula, $x(t)$ is the road displacement, $W(t)$ is the mean value of 0 Gaussian white noise, f_0 is the lower cutoff frequency, $n_0 = 0.1\ m^{-1}$, and $f_0 = 0.1$ Hz.

The basic idea of the model is to abstract the random fluctuations of the road process as white noise satisfying certain conditions, and then fit the time domain model of the random unevenness of the road by a hypothetical system with appropriate transformation. The pavement unevenness refers to the deviation of the road surface from the ideal plane. The rougher the pavement and the worse the pavement grade, the higher the geometric mean of power spectral density. In this paper, we simulate and analyze the A–D pavements, respectively, and the specific parameters are shown in Table 1.

Table 1. Parameters for each grade of pavement.

Road Grade	Geometric Mean of Power Spectral Density $G_q(n_0)/10^{-6}$ m^3
A	16
B	64
C	256
D	1024

2.2.2. Step Noise Road Excitation

The white noise pavement excitation is mainly used to simulate continuously uneven pavement, such as asphalt pavement, gravel road surface, etc. However, it is usually necessary to consider the response to an encountered shock in addition to the continuous vibration. Here, step pavement excitation is used for simulation. The specific mathematical expression is as follows:

$$x(t) = \begin{cases} 0, & t < t_1 \\ x, & t \geq t_1 \end{cases} \quad (7)$$

From the equation, x denotes the displacement of the step and t_1 denotes the time when the step occurs.

2.3. Controller Design Principle

2.3.1. FNN-PID Controller

The structure of the FNN-PID controller is shown in Figure 2.

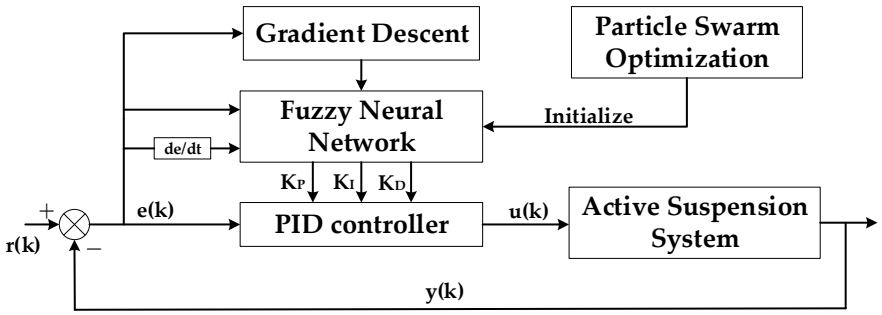

Figure 2. FNN-PID controller structure model.

In Figure 2, the input of the FNN is the deviation of Sprung Mass Acceleration, e(k), and the rate of change of deviation, de/dt; the input of the PID controller is e(k) [27] and u(k) is the control quantity. The anticipated value of the system is denoted by r(k), and the actual output value is denoted by y(k). After the fuzzy neural network algorithm has been trained, the best control parameters for the PID controller are obtained. According to the optimal control parameters, the PID controller enables real-time control of the suspension system by adjusting the magnitude of the control quantity, u(k).

2.3.2. PID Control

In the field of industrial automation control, the PID algorithm is a common control algorithm [28]. The discrete control rate of a commonly used PID algorithm is shown in Equation (8).

$$u(k) = K_p e(k) + K_i \sum_{i=0}^{k} e(i) + K_d[e(k) - e(k-1)] \quad (8)$$

In the formula, the error between the system's input and output is denoted as e(k); $K_i \sum_{i=0}^{k} e(i)$ is the cumulative sum of the error, and the error's rate of change is $e(k) - e(k-1)$.

In PID control, the proportional link is used to quickly eliminate the error between input and output; the larger the proportional coefficient, K_p, the faster the system response. The integral link is used to lower the system's static error; the larger the integral coefficient, K_i, the more accurate the system response. The differential link is used to eliminate the oscillation in the control process; the larger the differential coefficient, K_d, the more robust the system response process.

The control of the active suspension system often uses incremental PID control. According to Formulas (9) and (10), it can be seen that, when the three coefficients, K_p, K_i, and K_d, in the PID control are determined after only using the deviation measured before and after the moment to derive the control increment by the formula, the control amount corresponds to the increment of the last few errors. There is no accumulation of errors; only those related to the last three sampling values belong to the recursive algorithm.

$$\Delta u(k) = K_p[e(k) - e(k-1)] + K_i e(k) + K_d[e(k) - 2e(k-1) + e(k-2)] \quad (9)$$

$$u(k) = u(k-1) + \Delta u(k) \quad (10)$$

2.3.3. FNN Control

The structure of the FNN is displayed in Figure 3, and it is split into five layers, including input layer, fuzzification layer, fuzzy inference layer, normalization layer, and output layer.

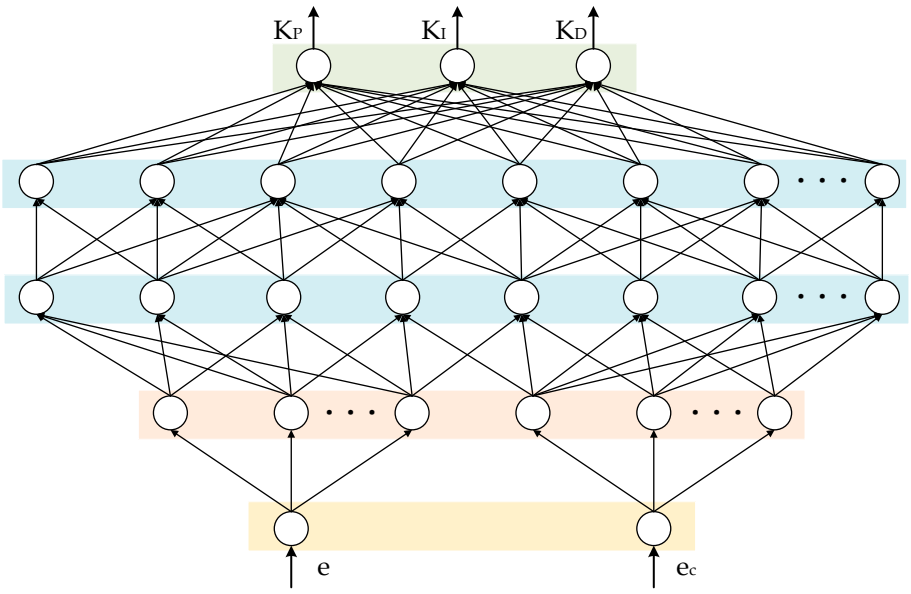

Figure 3. FNN structure model.

Input layer: the vector of input is $x = [x_1, x_2, \cdots, x_n]$. The nodes of this layer of the network are directly connected to each component, x_i, and the error, e(k), and the error rate of change, $e_c(k)$, are the inputs to the general FNN. The result of the first layer is y_i^1.

$$y_i^1 = x_i, i = 1, 2, \cdots, n \quad (11)$$

Fuzzification layer: Each neuron in this layer represents 1 Gaussian subordinate function, whose role is to divide the input values into fuzzy intervals and fuzzy them [29]. The output is represented as follows:

$$y_{ij}^2 = \exp\left[\frac{\left(u_{ij} - c_{ij}\right)^2}{{b_{ij}}^2}\right] \tag{12}$$

In the formula, $i = 1, 2, \cdots, n$, $j = 1, 2, \cdots, m_i$, the quantity of input vectors is n, and the number of fuzzy rules is m_i. The Gaussian function's center and width, respectively, are denoted by c_{ij} and b_{ij}. The output quantity is expressed as y_{ij}^2.

Fuzzy inference layer: A fuzzy rule from the fuzzy rule base is represented by each neuron. The aim is to determine each rule's fitness, and the common calculation methods are the minimum value method and the product method. The product method is chosen here for calculation.

$$y_h^3 = x_1^{i_1} \cdot x_2^{i_2} \cdots x_m^{i_n} \tag{13}$$

In the formula, $i_j = 1, 2, \cdots, m_i$, $h = 1, 2, \cdots, m$, $m = \prod_{j=1}^{n} m_j$.

Normalization layer: The output of the fuzzy inference layer is normalized. The quantity of nodes in this layer is equal to the amount of nodes in the fuzzy inference layer, and the output of the normalization layer is as stated below.

$$y_h^4 = \frac{y_h^3}{\sum_{h=1}^{m} y_h^3} \tag{14}$$

Output layer: This layer uses the center of gravity approach to realize the clarification and defuzzification process, and the output obtained after calculation is the result of PID parameter adjustment.

$$y_k = \sum_{h=1}^{m} y_h^4 \omega_s^j = \sum_{h=1}^{m} \frac{y_h^3}{\sum_{h=1}^{m} y_h^3} \omega_s^j \tag{15}$$

In the formula, in the fuzzy inference layer, there are m nodes, $k = 1, 2, \cdots, r$; the output layer's node count is denoted by the symbol r, and ω_s^j is the jth weight corresponding to the sth output.

2.3.4. FNN Optimization Algorithm

The learning optimization strategy of FNN is usually to continuously adjust the parameters of the network by the gradient descent method to obtain the ideal control parameters. Determining the best learning parameters and avoiding local optimality can be accomplished using a particle swarm algorithm (PSO) to solve continuous and discrete optimization problems [30,31]. However, the optimization speed of PSO is not very quick, its local search performance is subpar, and it is simple to fall into a local extremum. In general, the PSO method is very slow in searching around the global optimum. To address the shortcomings of existing optimization algorithms, the gradient descent algorithm and PSO algorithm are combined to optimize the network parameters. The approximate optimal solutions of the network weight parameters are found by using the particle swarm algorithm's global search capability, after which they are adjusted and optimized using the gradient descent approach, thus improving the training accuracy of the fuzzy neural network.

1. Gradient Descent;

The network weight learning error metric is defined as:

$$E(k) = \frac{1}{2} e(k)^2 = \frac{1}{2} [r(k) - y(k)]^2 \tag{16}$$

From the gradient descent method, the learning algorithm of the network is expressed as [32]:

$$\Delta\omega_s^j(k) = -\eta\frac{\partial E(k)}{\partial \omega_s^j} \tag{17}$$

$$\omega_s^j(k) = \omega_s^j(k-1) + \Delta\omega_s^j(k) + \alpha\left[\omega_s^j(k-1) - \omega_s^j(k-2)\right] \tag{18}$$

where η is the learning rate, α is the momentum factor, and $\eta \in [0,1]$, $\alpha \in [0,1]$.

The same can be obtained:

$$c_{ij}(k) = c_{ij}(k-1) + \Delta c_{ij}(k) + \alpha\left[c_{ij}(k-1) - c_{ij}(k-2)\right] \tag{19}$$

$$b_{ij}(k) = b_{ij}(k-1) + \Delta b_{ij}(k) + \alpha\left[b_{ij}(k-1) - b_{ij}(k-2)\right] \tag{20}$$

2. Particle swarm algorithm

The population intelligence optimization approach designated as particle swarm optimization (PSO) is frequently employed in multi-objective optimization situations [33,34]. The specific working process is as follows: Suppose a particle swarm with M particles searches for the optimal position in a space of N dimensions. Assuming that the position of the ith particle (i =1, 2, . . . , M) is x_i and the velocity is v_i, the individual extreme value, p_{ibest}, and the group extreme value, p_{gbest}, of the particle are determined according to the particle fitness value, and the particle is continuously updated according to p_{ibest} and p_{gbest}. Its own position and velocity are updated to find the global optimal solution. The particle velocity and position update formulas are expressed as:

$$v_{id}^{t+1} = \omega v_{id}^t + c_1 r_1\left(p_{ibestd}^t - x_{id}^t\right) + c_2 r_2\left(p_{gbestd}^t - x_{id}^t\right) \tag{21}$$

$$x_{id}^{t+1} = x_{id}^t + v_{id}^{t+1} \tag{22}$$

In the formula, ω is the inertia weight, t is the number of current iteration steps, c_1 and c_2 are learning factors, r_1 and r_2 are random numbers between 0 and 1, and $d = 1, 2, \cdots, D$; $i = 1, 2, \cdots, M$.

2.3.5. Hybrid Algorithm Optimization Process

The hybrid algorithm of the particle swarm algorithm and gradient descent method to optimize the fuzzy neural network PID controller is denoted as PSO-FNN-PID. The specific steps of the hybrid algorithm to optimize the fuzzy neural network are shown in Figure 4.

1. The fuzzy neural network parameters, $c_{ij}, b_{ij}, \omega_s^j$, are initialized;
2. Particle swarm initialization. Parameters such as those of population size, particle dimensions, and initial inertia weight, as well as learning factor, are set first, after which a set of particle positions is generated at random and the particle's maximum and minimum velocities are determined; between the extremes of highest and minimum velocity, each particle's velocity is determined randomly;
3. After updating the velocity and position of the particle, the fitness value of the particle at each iteration step is calculated, and the individual optimal extremum, p_{ibest}, and the population optimal extremum, p_{gbest}, are updated;
4. If the termination condition is satisfied, the corresponding network parameters are passed to the FNN;
5. The FNN acquires the initial values of the parameters and then calculates them and updates the network parameters online by back-propagation through the gradient descent method. The final optimal solutions are output.

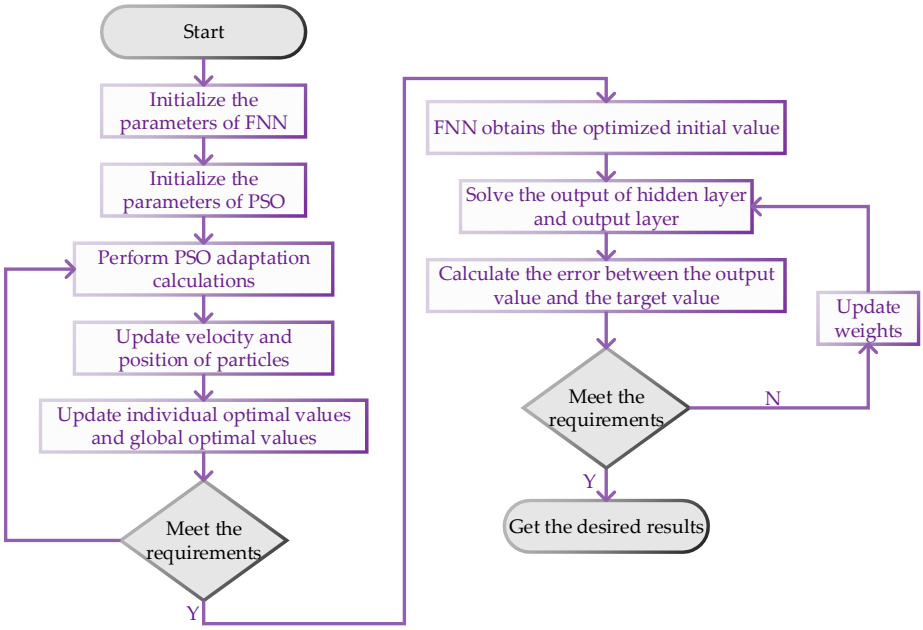

Figure 4. Hybrid algorithm optimization flow chart.

3. Results

Simulation of the models was performed using MATLAB/Simulink. According to the differential equations of motion and the 1/4 suspension system's stochastic road input model, the simulation models of the 1/4 active and passive suspension systems were created in Simulink. Table 2 illustrates the fundamental parameters for the 1/4 suspension model.

Table 2. Fundamental data of suspension system.

Variable	Value
Sprung mass M/kg	240
Unsprung mass m/kg	30
Tire stiffness K_1/(N/m)	160,000
Spring rate K_2/(N/m)	16,000
Suspension damping c/(N•s)/m	980

For the sake of highlighting the optimization effect of the FNN-PID control strategy and to verify its effectiveness, the passive suspension, PID, and FNN-PID control active suspension were emulated and analyzed, respectively. The PID controller's parameters were $K_P = 5$, $K_I = 430$, and $K_D = 0.1$. The structure of the FNN was designed as 2-14-49-49-3, and the number of network parameters to be adjusted was $14 \times 2 + 49 \times 3 = 175$. Therefore, the dimension of the particles is set to 175, and then the following other pertinent settings are made to the particle swarm algorithm: the overall population size is 150, the learning factor is c1 = c2 = 2, and the inertia weight is 0.8. The particle velocity interval for the width of the affiliation function, b_{ij}, and the center value, c_{ij}, is set to $[-3, 3]$, and the particle velocity interval for the connection weight, ω_s^j, of the FNN is $[-1, 1]$. The learning rate of the FNN is $\eta = 0.5$ and the momentum factor is $\alpha = 0.2$.

When vehicles are driven on actual highways and dirt roads, they are often subjected to impact-type road surfaces, such as gravel and speed bumps, which affect all vehicle driving performance. In order to study the control effect of the FNN-PID-controlled active suspension under such operating conditions, a stepped road model was established to examine the vibration response properties of the suspension under such conditions. The step excitation with a step amplitude of 0.01 m was selected, as well as the suspension system's vibration response curve, which is displayed in Figures 5–7.

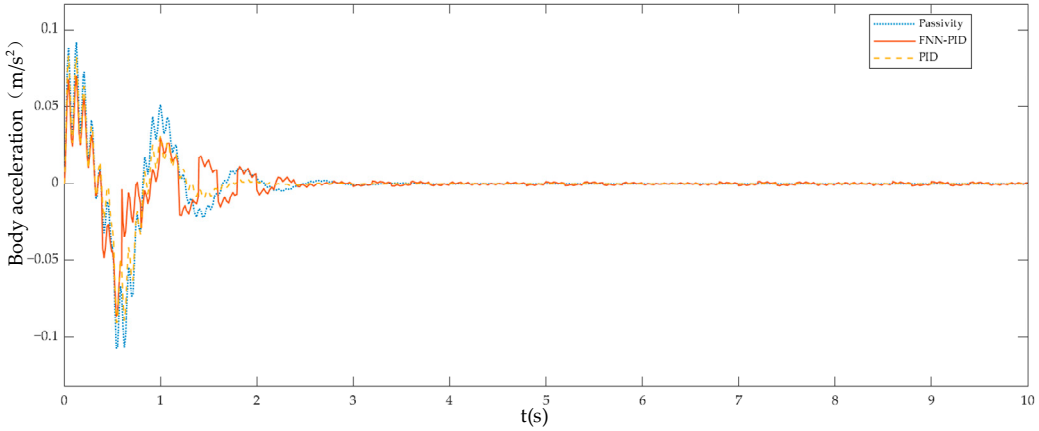

Figure 5. Step response diagram of Sprung Mass Acceleration.

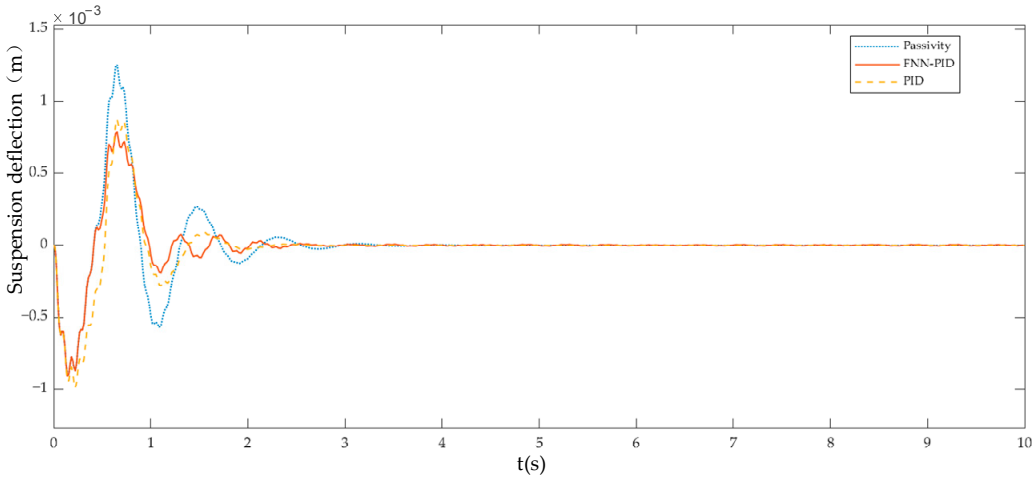

Figure 6. Step response diagram of Dynamic Deflection of Suspension.

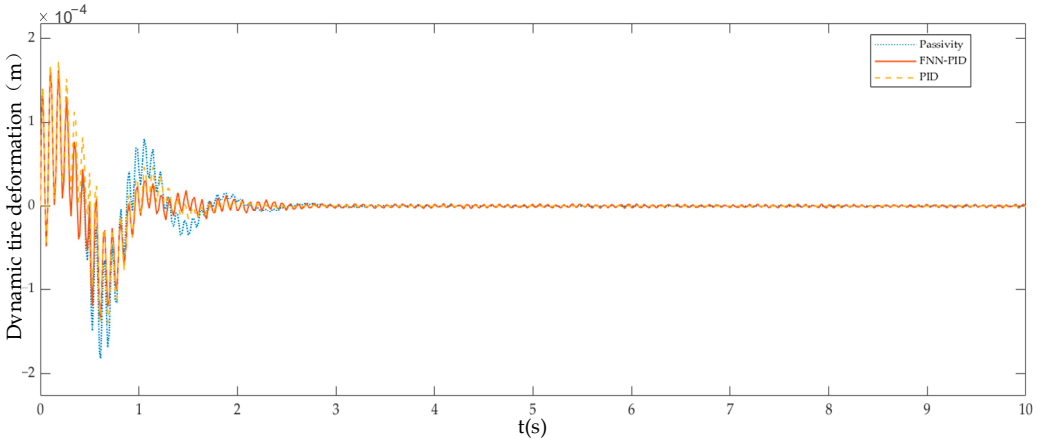

Figure 7. Step response diagram of Dynamic Tire Deformation.

Figure 5 demonstrates that the vehicle suspension system with the FNN-PID controller has better Sprung Mass Acceleration (SMA) than the conventional suspension system, which can make the body more stable with good control effect and can make the vehicle amplitude stable in a short time and quickly converge to 0. Additionally, Figures 6 and 7 show that the Dynamic Deflection of Suspension (DDS) and Dynamic Tire Deformation (DTD) can also reduce the amplitude under FNN-PID control and cause it to quickly converge to 0. Therefore, the active suspension controlled by FNN-PID can effectively reduce vibration and recover quickly, which greatly improves the passenger's ride experience.

Meanwhile, Table 3 shows the root mean square of each suspension index, demonstrating that the SMA, DDS, and DTD of the active suspension system with the FNN-PID controller are improved to some extent. The SMA, DDS, and DTD are decreased by 30.7%, 23.4%, and 16.3%, respectively, when compared to passive suspension. Compared to the PID-controlled active suspension system, the three performance indicators are reduced by 14.6%, 11.3%, and 8.2% respectively. The FNN-PID controller clearly has the potential to significantly lower the suspension's performance indices and improve the vehicle's passenger comfort.

Table 3. Comparison of root-mean-square suspension performance under step excitation.

Index	Passive	PID Controller	FNN-PID Controller
SMA (m/s^2)	2.265×10^{-2}	1.838×10^{-2}	1.570×10^{-2}
DDS (m)	2.896×10^{-4}	2.502×10^{-4}	2.219×10^{-4}
DTD (m)	3.671×10^{-5}	3.350×10^{-5}	3.074×10^{-5}

In addition, the issue of the time between the change in road conditions and the response achieved by the suspension system is taken into account. A set of control tests was set up with the objective of achieving a steady state of vehicle vertical displacement under step response. As shown in Figure 8, the suspension is given a step signal of 0.01 m, 0.05 m, and 0.08 m at 1 s, and a reasonable steady-state error, Δ, is set. When the step signal is 0.01 m, $\Delta = 0.0002$, and when the step signal is 0.05 m and 0.08 m, $\Delta = 0.001$. When the step signal is 0.01 m and 0.05 m, the time for the FNN-PID controller to reach steady state is approximately 2.1 s, and the overall response time is 1.1 s. The time for the PID controller to reach steady state is approximately 2.4 s, with an overall response time of 1.4 s, and the passive system reaches steady state in approximately 3.1 s, with an overall response time of 2.1 s. When the step signal is 0.08, the time for the FNN-PID controller to reach steady-state is approximately 2.6 s, and the overall response time is 1.6 s. The time for the PID controller to reach steady-state is approximately 2.7 s, the overall response time is 1.7 s, and the passive system reaches steady state in approximately 3.4 s, with an overall response time of 2.4 s. The results show that the response time of the FNN-PID controller is reduced by 21.4% compared to the PID controller and 47.6% compared to the passive suspension when the road conditions are less variable. When the road conditions vary widely, the response time of the FNN-PID controller is reduced by only 5.9% compared to the PID controller and 33.3% compared to the passive suspension.

In order to obtain each suspension performance index under normal vehicle driving, the proposed random road excitation is used for simulation analysis. It is assumed that the vehicle is driven in a straight line at 30 km/h on the Class B road, with a simulation time of 20 s. The simulation is performed under the control of the PID controller and FNN-PID controller, respectively. The SMA, DDS, and DTD were still chosen as the main indexes to evaluate the performance of suspension, and the simulation result curves are shown in Figures 9–11.

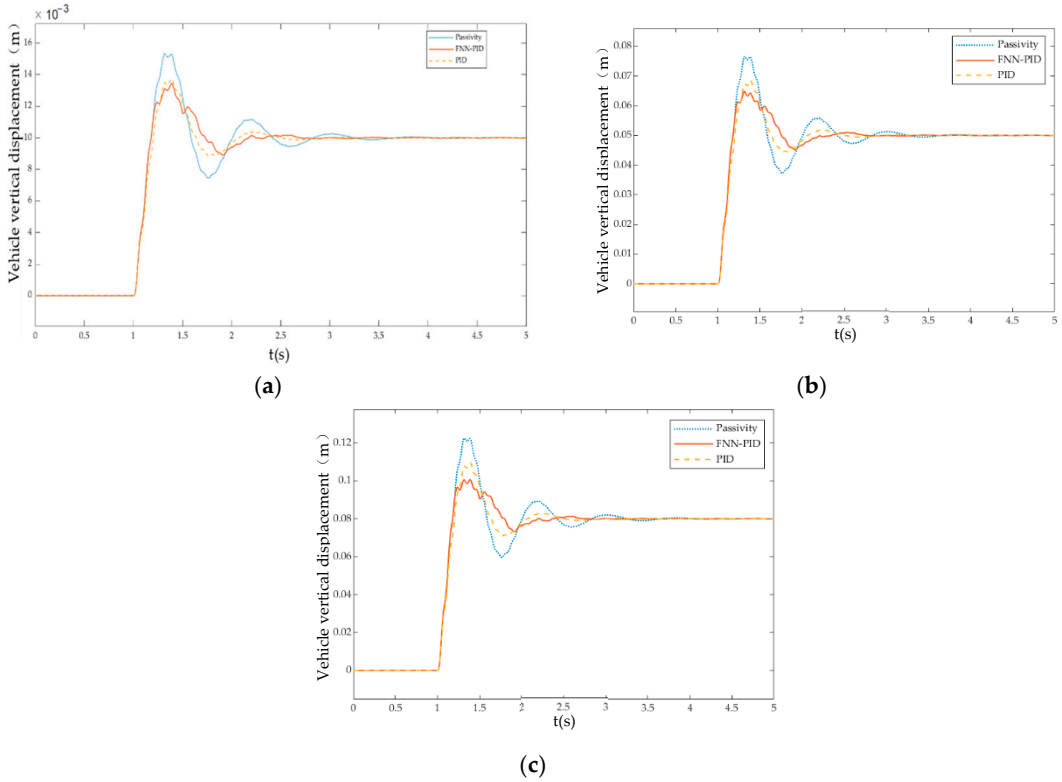

Figure 8. Plot of vehicle vertical displacement change under step signal. (**a**) The step signal is 0.01 m. (**b**) The step signal is 0.05 m. (**c**) The step signal is 0.08 m.

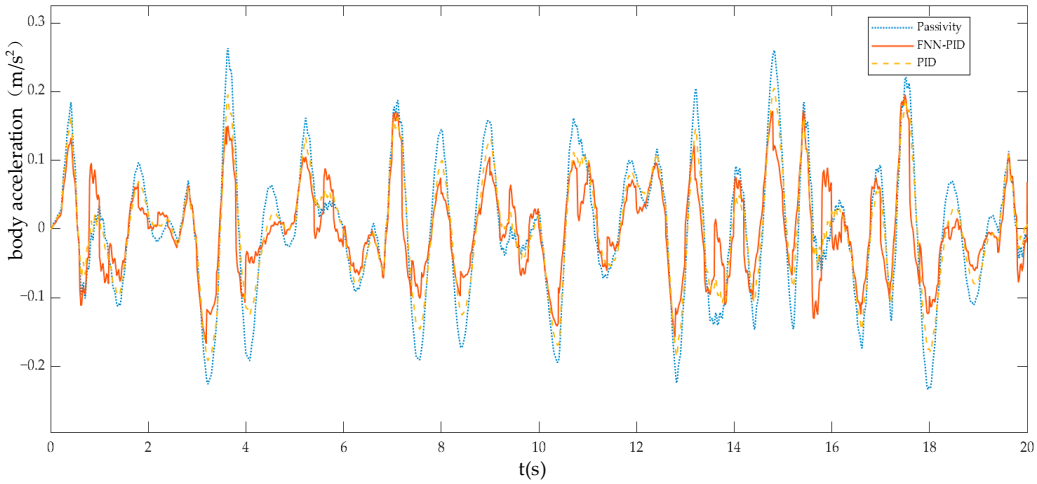

Figure 9. Comparison of Sprung Mass Acceleration simulation results.

From Figures 9–11, it is clear that, in comparison with the passive suspension system, the SMA, DDS, and DTD of the active suspension system with the PID controller and the FNN-PID controller are reduced to a certain extent, indicating that both designed active suspension control systems are able to curb the overall vehicle vibration.

To make the analysis of the control effect of different controllers on the suspension system more intuitive, the above graphs were data processed to obtain the root mean square values of each curve, as demonstrated in Table 4.

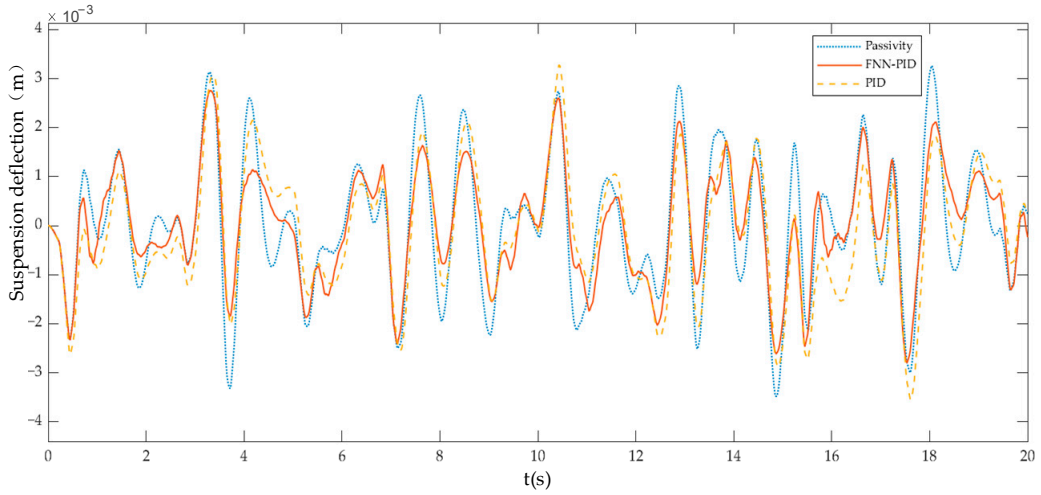

Figure 10. Comparison of Dynamic Deflection of Suspension simulation results.

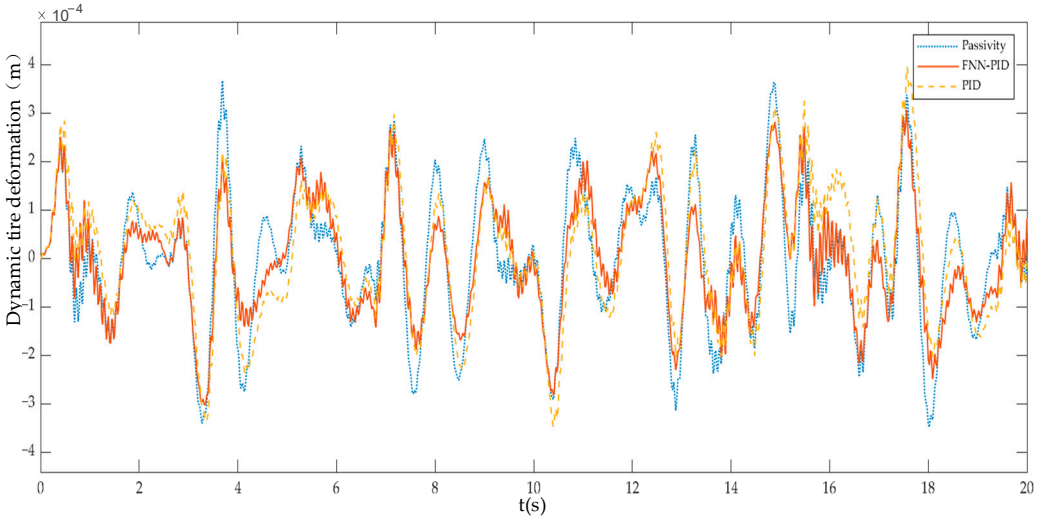

Figure 11. Comparison of Dynamic Tire Deformation simulation results.

Table 4. Root mean square comparison of suspension performance indexes under random.

Class	Index	Passive	PID Controller	FNN-PID Controller
A	SMA (m/s^2)	0.0490	0.0391	0.0334
	DDS (m)	6.735×10^{-4}	6.286×10^{-4}	5.525×10^{-4}
	DTD (m)	7.017×10^{-5}	6.701×10^{-5}	5.890×10^{-5}
B	SMA (m/s^2)	0.0979	0.0782	0.0681
	DDS (m)	1.346×10^{-3}	1.254×10^{-3}	1.107×10^{-3}
	DTD (m)	1.402×10^{-4}	1.336×10^{-4}	1.185×10^{-4}
C	SMA (m/s^2)	0.1820	0.1440	0.1257
	DDS (m)	2.515×10^{-3}	2.319×10^{-3}	2.012×10^{-3}
	DTD (m)	2.576×10^{-4}	2.508×10^{-4}	2.151×10^{-4}
D	SMA (m/s^2)	0.3476	0.2673	0.2390
	DDS (m)	4.747×10^{-3}	4.354×10^{-3}	3.820×10^{-3}
	DTD (m)	4.933×10^{-4}	4.602×10^{-4}	4.003×10^{-4}

Table 4 illustrates that, in comparison with the passive suspension, the active suspension with FNN-PID control has 30.4%, 17.8%, and 15.5% reduction in SMA, DDS, and DTD,

respectively. On the other hand, the SMA, DDS, and DTD of the active suspension with FNN-PID control were reduced by 14.6%, 12.1%, and 11.2%, respectively, compared to the active suspension with PID control. From these data, it is possible to draw the conclusion that, when compared with the other two suspension systems, the FNN-PID controller is able to suppress the variation of SMA, so that the wheels can closely follow the road, ensuring good maneuverability while giving passengers a more comfortable ride.

4. Discussion

A 1/4 active suspension simulation model was established in MATLAB/Simulink, and a PSO-FNN-PID control algorithm was designed. By combining the PSO algorithm and the gradient descent method, the initial parameters of the FNN were optimized offline and then finetuned online, so as to obtain the optimal control rules and realize the real-time online adjustment of the PID control parameters. The combination of the two methods allowed the learning process to avoid falling into local minima while reaching the exact value at a later stage of learning. The simulation analysis indicated that the active suspension system with PSO-FNN-PID control had a preferable control effect compared with the passive suspension system and active suspension system with PID control, and could effectively attenuate the body vibration caused by external disturbance. Therefore, an examination of the graphs and data reveals that the PSO-optimized FNN-PID controller has significantly superior performance, and is capable of enhancing the vehicle's road adhesion and ensuring a smooth and comfortable ride. In the future, we will continue to explore the possibility of implementing this control system in the whole vehicle system and consider the development and implementation of related hardware and software. In addition, we also hope to make some changes to the basic PID control, such as including an integral anti-saturation control strategy, in order to obtain better results.

Author Contributions: Conceptualization, M.L. and J.L.; methodology, M.L.; software, J.L.; validation, J.L. and J.X.; formal analysis, J.L.; investigation, G.L.; resources, M.L.; data curation, J.L.; writing—original draft preparation, G.L.; writing—review and editing, M.L.; visualization, J.X.; supervision, M.L.; funding acquisition, M.L. All authors have read and agreed to the published version of the manuscript.

Funding: This research was funded by Natural Science Foundation of Hainan Province, grant number 2019RC144, and supported by China Scholarship Council, grant number 202007565009.

Data Availability Statement: Not applicable.

Conflicts of Interest: The authors declare no conflict of interest.

References

1. Manolache-Rusu, I.-C.; Suciu, C.; Mihai, I. Analysis of Passive vs. Semi-Active Quarter Car Suspension Models. In *Advanced Topics in Optoelectronics, Microelectronics and Nanotechnologies X*; SPIE: Bellingham, WA, USA, 2020; Volume 11718, p. 117181Q. [CrossRef]
2. Kumar, S.; Medhavi, A.; Kumar, R. Active and Passive Suspension System Performance under Random Road Profile Excitations. *Int. J. Acoust. Vib.* **2020**, *25*, 532–541. [CrossRef]
3. Babawuro, A.Y.; Tahir, N.M.; Muhammed, M.; Sambo, A.U. Optimized State Feedback Control of Quarter Car Active Suspension System Based on LMI Algorithm. *J. Phys. Conf. Ser.* **2020**, *1502*, 012019. [CrossRef]
4. Haemers, M.; Derammelaere, S.; Ionescu, C.-M.; Stockman, K.; De Viaene, J.; Verbelen, F. Proportional-Integral State-Feedback Controller Optimization for a Full-Car Active Suspension Setup Using a Genetic Algorithm. *IFAC-PapersOnLine* **2018**, *51*, 1–6. [CrossRef]
5. Youness, S.F.; Lobusov, E.C. Networked Control for Active Suspension System. *Procedia Comput. Sci.* **2019**, *150*, 123–130. [CrossRef]
6. Nguyen, T.A. Control an Active Suspension System by Using PID and LQR Controller. *Int. J. Mech. Prod. Eng. Res. Dev.* **2020**, *10*, 7003–7012. [CrossRef]
7. Bai, R.; Wang, H.-B. Robust Optimal Control for the Vehicle Suspension System with Uncertainties. *IEEE Trans. Cybern.* **2021**, *52*, 9263–9273. [CrossRef] [PubMed]
8. Jibril, M.; Alluvada, P. Quarter Car Active Suspension System Design Using Optimal and Robust Control Method. *Ind. Eng. Lett.* **2020**, *10*, 43.

9. Li, Z. Evaluating Car's Ride Comfort and Controlling Vibration of Suspension System Based on Adaptive PID Control. *Tech. J. Daukeyev Univ.* **2021**, *1*, 1–9. [CrossRef]
10. Li, Z.; Chen, L.; Zheng, Q.; Dou, X.; Yang, L. Control of a Path Following Caterpillar Robot Based on a Sliding Mode Variable Structure Algorithm. *Biosyst. Eng.* **2019**, *186*, 293–306. [CrossRef]
11. Saifi, D.; Kumar, P. Modelling of Active Suspension System for Quarter Car (PID Control, MATLAB). *Int. J. Eng. Appl. Sci. Technol.* **2021**, *5*, 155–160. [CrossRef]
12. Khodadadi, H.; Ghadiri, H. Self-Tuning PID Controller Design Using Fuzzy Logic for Half Car Active Suspension System. *Int. J. Dyn. Control* **2018**, *6*, 224–232. [CrossRef]
13. Cao, K.; Li, Z.; Gu, Y.; Zhang, L.; Chen, L. The Control Design of Transverse Interconnected Electronic Control Air Suspension Based on Seeker Optimization Algorithm. *Proc. Inst. Mech. Eng. Part D J. Automob. Eng.* **2021**, *235*, 2200–2211. [CrossRef]
14. Muderrisoğlu, K.; Arisoy, D.O.; Ahan, A.O.; Akdogan, E. PID Parameters Prediction Using Neural Network for A Linear Quarter Car Suspension Control. *Int. J. Intell. Syst. Appl. Eng.* **2016**, *4*, 20–24. [CrossRef]
15. Wang, M.; Pang, H.; Wang, P.; Luo, J. BP Neural Network and PID Combined Control Applied to Vehicle Active Suspension System. In Proceedings of the 2021 40th Chinese Control Conference (CCC), Shanghai, China, 26–28 July 2021; pp. 8187–8192.
16. Qiu, R. Adaptive Control of Vehicle Active Suspension Based on Neural Network Optimization. *E3S Web Conf.* **2021**, *261*, 03046. [CrossRef]
17. Ahmed, A.A.; Saleh Alshandoli, A.F. Using Of Neural Network Controller and Fuzzy PID Control To Improve Electric Vehicle Stability Based On A14-DOF Model. In Proceedings of the 2020 International Conference on Electrical Engineering (ICEE), Istanbul, Turkey, 28–27 September 2020; pp. 1–6.
18. Han, S.-Y.; Dong, J.-F.; Zhou, J.; Chen, Y.-H. Adaptive Fuzzy PID Control Strategy for Vehicle Active Suspension Based on Road Evaluation. *Electronics* **2022**, *11*, 921. [CrossRef]
19. Swethamarai, P.; Lakshmi, P. Adaptive-Fuzzy Fractional Order PID Controller-Based Active Suspension for Vibration Control. *IETE J. Res.* **2022**, *68*, 3487–3502. [CrossRef]
20. Sadeghi, M.S.; Varzandian, S.; Barzegar, A. Optimization of Classical PID and Fuzzy PID Controllers of a Nonlinear Quarter Car Suspension System Using PSO Algorithm. In Proceedings of the 2011 1st International Conference on Computer and Knowledge Engineering (ICCKE), Mashhad, Iran, 13–14 October 2011; pp. 172–176.
21. Gandhi, P.; Adarsh, S.; Ramachandran, K.I. Performance Analysis of Half Car Suspension Model with 4 DOF Using PID, LQR, FUZZY and ANFIS Controllers. *Procedia Comput. Sci.* **2017**, *115*, 2–13. [CrossRef]
22. Shalabi, M.E.; Fath Elbab, A.M.R.; El-Hussieny, H.; Abouelsoud, A.A. Neuro-Fuzzy Volume Control for Quarter Car Air-Spring Suspension System. *IEEE Access* **2021**, *9*, 77611–77623. [CrossRef]
23. Pang, H.; Liu, F.; Xu, Z. Variable Universe Fuzzy Control for Vehicle Semi-Active Suspension System with MR Damper Combining Fuzzy Neural Network and Particle Swarm Optimization. *Neurocomputing* **2018**, *306*, 130–140. [CrossRef]
24. Ghosh, G.; Mandal, P.; Mondal, S.C. Modeling and Optimization of Surface Roughness in Keyway Milling Using ANN, Genetic Algorithm, and Particle Swarm Optimization. *Int. J. Adv. Manuf. Technol.* **2019**, *100*, 1223–1242. [CrossRef]
25. Zhao, Q.; Zhu, B. Multi-Objective Optimization of Active Suspension Predictive Control Based on Improved PSO Algorithm. *J. Vibroeng.* **2019**, *21*, 1388–1404. [CrossRef]
26. Yuan-chun, K. Fatigue Analysis of Suspension Control Arm Based on Road Spectrum. *IOP Conf. Ser. Mater. Sci. Eng.* **2019**, *538*, 012062. [CrossRef]
27. Zhou, Z.C.; Chen, R. Design on Fuzzy Neural Network PID Control System of Diesel Engine. *Adv. Mater. Res.* **2013**, *756–759*, 425–429. [CrossRef]
28. Borase, R.P.; Maghade, D.K.; Sondkar, S.Y.; Pawar, S.N. A Review of PID Control, Tuning Methods and Applications. *Int. J. Dyn. Control* **2021**, *9*, 818–827. [CrossRef]
29. Cao, P.; Zhao, W.; Liu, S.; Shi, L.; Gao, H. Using a Digital Camera Combined with Fitting Algorithm and T-S Fuzzy Neural Network to Determine the Turbidity in Water. *IEEE Access* **2019**, *7*, 83589–83599. [CrossRef]
30. Jain, N.K.; Nangia, U.; Jain, J. A Review of Particle Swarm Optimization. *J. Inst. Eng. India Ser. B* **2018**, *99*, 407–411. [CrossRef]
31. Bansal, J.C. Particle Swarm Optimization. In *Evolutionary and Swarm Intelligence Algorithms*; Bansal, J.C., Singh, P.K., Pal, N.R., Eds.; Studies in Computational Intelligence; Springer International Publishing: Cham, Switzerland, 2019; pp. 11–23, ISBN 978-3-319-91341-4.
32. Dogo, E.M.; Afolabi, O.J.; Nwulu, N.I.; Twala, B.; Aigbavboa, C.O. A Comparative Analysis of Gradient Descent-Based Optimization Algorithms on Convolutional Neural Networks. In Proceedings of the 2018 International Conference on Computational Techniques, Electronics and Mechanical Systems (CTEMS), Belgaum, India, 21–22 December 2018; pp. 92–99.
33. Lv, S.; Chen, G.; Dai, J. Active Suspension Control Based on Particle Swarm Optimization. *Recent Pat. Mech. Eng.* **2020**, *13*, 60–78. [CrossRef]
34. Bejarbaneh, E.Y.; Bagheri, A.; Bejarbaneh, B.Y.; Buyamin, S.; Chegini, S.N. A New Adjusting Technique for PID Type Fuzzy Logic Controller Using PSOSCALF Optimization Algorithm. *Appl. Soft Comput.* **2019**, *85*, 105822. [CrossRef]